

CONTENTS

(Section 6)

	Page
6. REACTOR CORE.....	6-1
6.1. Reactor Core Description.....	6-1
6.1.1. General Description.....	6-1
6.1.2. Fuel Elements.....	6-2
6.1.3. Control Rods.....	6-3
6.1.4. Internals.....	6-5
6.1.5. Shuffled Core.....	6-8
6.2. Thermal and Hydraulic Design.....	6-8
6.2.1. Design Criteria.....	6-8
6.2.2. Hydraulic Performance.....	6-9
6.2.3. Thermal Performance.....	6-9
6.2.4. Burnout.....	6-11
6.3. Nuclear Characteristics.....	6-13
6.3.1. Core Description.....	6-14
6.3.2. Reactivity Coefficients.....	6-17
6.4. Shipboard Physics Test Program.....	6-24
6.4.1. Program Objectives.....	6-24
6.4.2. Nuclear Instrumentation Calibration.....	6-27
6.4.3. Reactivity Coefficients.....	6-29
6.4.4. Control Rods.....	6-33
6.4.5. Transient Tests.....	6-36
6.4.6. Xenon Buildup to Equilibrium.....	6-36

List of Tables

Table

6-1. Core Design Characteristics.....	6-1
6-2 Thermal and Hydraulic Characteristics.....	6-9
6-3 Core Ia Nuclear Characteristics.....	6-15
6-4. Volume Fractions and Number Densities, Unit Fuel Rod Cell.....	6-16
6-5 Calculated Core I Doppler Coefficient of Reactivity and Total Reactivity Deficit.....	6-19
6-6 Measured Core I Power Doppler Coefficient From Uncontrolled Transients at 2335 EFPH.....	6-19
6-7 Measured Operating Coefficients.....	6-23
6-8 Sequence of the 1399 and 3079 EFPH Physics Test.....	6-25

6. REACTOR CORE

6.1. Reactor Core Description

6.1.1. General Description

The reactor core comprises the fuel elements, the control rods, and the reactor vessel internals. Each of these is described in detail below. The core (see Drawing SK13-G-865) is cooled by the primary coolant, which flows through the thermal shields, through the second-pass fuel elements, and finally through the third-pass fuel elements. The core design characteristics are summarized in Table 6-1.

Table 6-1. Core Design Characteristics

<u>Characteristic</u>	<u>Design parameter</u>
<u>Core dimensions</u>	
Core overall length, in.	90.24
Active fuel length, in.	66
Equivalent core diameter, in.	62.06
<u>Fuel element containers</u>	
Number	32
Material	Type 304 stainless steel
Outside dimension, in.	8.988
Second-pass wall thickness, in.	0.109
Third-pass wall thickness, in.	0.094
Pitch spacing, in.	9.723
<u>Fuel elements</u>	
Type	Brazed ferrule
Number	32
Length overall, in.	73-5/8
Width, in.	8.456
Number of rods per element	164
Element pitch spacing, in.	9.723

Table 6-1. (Cont'd)

<u>Characteristic</u>	<u>Design parameter</u>
<u>Main spacer ferrules</u>	
Material	Type 304 stainless steel
OD, in.	0.4375
Wall thickness, in.	0.020
Length, in.	1.0
<u>Peripheral ferrules</u>	
Material	Type 304 stainless steel
OD, in.	0.234
Wall Thickness, in.	0.018
Length, in.	1.0
Braze material	90% Ni and 10% P
<u>Fuel rods</u>	
Material	Type 304 stainless steel
Number of fuel rods in core	5248
Length, in.	69
OD, in.	0.500
Wall thickness, in.	0.035
Pitch, in.	0.663
<u>Fuel pellets</u>	
Material	UO ₂
Density, % of theoretical	93 ²
Diameter, in.	0.4245
Pellet-to-fuel-rod diametrical clearance, maximum, cold, in.	0.007

6.1.2. Fuel Elements

The active region of the NS Savannah core contains 32 fuel elements. There are 16 fuel elements in the downflow or second pass, and 16 in the upflow of third pass.

Each fuel element (shown in Figure 6-1 and Drawing SK13-G-864) is an integrally welded and brazed unit about 8-1/2 inches square and 76-1/2 inches long. The fuel element is designed to withstand shocks from ship motion, vibration from water flow, thermal distortion caused by nuclear heating, and loadings that occur in handling, shipping and manufacturing. Each fuel element is composed of four subassemblies, which are six-by-seven arrays of fuel rods in a square matrix.

Each fuel rod (see Figure 6-2) is a 69-inch-long stainless steel tube having an outside diameter of 0.500 inch and a wall thickness of 0.035 inch. The rods are loaded with UO_2 pellets (0.4245 inch in diameter) which are sintered to a minimum of 93% of theoretical density. The pellets are held in the tubes by welded end plugs, and the gap between the tube and the pellets contains helium, which is introduced during the end-plug welding process. There are 164 fuel rods per element, making a total of 5248 rods in the entire core. The rods are on 0.663-inch centers. The active fuel length is 66 inches, leaving a clearance of about 2 inches to accommodate differential thermal expansion of the fuel within the tube.

The fuel tubes are secured in a square lattice by stainless steel ferrules brazed to the tube walls. These ferrules are spaced along the length of the fuel bundle in nine separate planes approximately 8 inches apart.

A supporting frame at each end of the fuel element attaches the four subassemblies into an integral assembly. The frame is designed to maintain structural stability with a minimum amount of flow interference. The lower frame mates with a self-centering seating surface on the lower transition piece of the fuel container assembly, serving to align and support the fuel element. The upper frame acts as a seat for the fuel element nozzles. The fuel element nozzle is sealed against the upper grid plate, and the nozzle helps to hold the fuel element in place under conditions of pitch and roll. As shown in Drawing SK13-G-864, a cylindrical shaft extends along the full length of each fuel element. A handling knob, attached to this shaft, permits lifting and handling the fuel element and also provides a receptacle for the two startup neutron sources.

6.1.3. Control Rods

The control rod and follower assembly (see Drawing

SK13-G-863) consists of three sections: a stainless steel extension, a neutron-absorbing portion, and a Zircaloy-2 follower rod. All three sections are rigidly fastened together in a continuous assembly. There are 21 cruciform control rods arranged on a square pitch.

The absorbing section of the control rod has a center of stainless steel and 1.7% boron. The boron is enriched to 92% B-10. The absorbing section is incased in a type 304 stainless steel sheath. This stainless steel sheath acts as the structural member for this portion of the control rod and eliminates dependence upon the neutron-absorbing material for load-carrying characteristics. The absorbing section is held together by dowels plug-welded to the sheath on each side of the boron-and-stainless-steel insert. The dowels are designed with small, sharp fins centered in slightly oversized holes bored through the composite assembly. In operation, if differential expansion should occur between the boron-and-stainless-steel insert and the stainless steel sheath, the dowel fins would deform and eliminate excessive stresses on the assembly itself.

The follower rod is made up of Zircaloy-2 angles spot-welded together to form a cruciform cross section. It is fastened to the neutron-absorbing section by a flush lap joint using plug-welded rivets. Longitudinal slots, extending beyond the length of the lap joint, are cut into Zircaloy between the rows of rivets to allow for the difference in expansion between the stainless steel and the Zircaloy at the joint. The stainless steel extension on the upper end of the control rod assembly replaces the boron-containing stainless steel. This section is above the active core, where the neutron-absorbing material is not required. The extension section is fastened to the control rod assembly by a lap joint employing plug-welded rivets. The drive line coupling is fastened to the upper end of the extension with dowels, which are welded in place.

The hub of the follower rod is filled with formed aluminum oxide to displace the water and thus reduce neutron flux peaking. The aluminum oxide gives better nuclear characteristics than those obtained from a solid Zircaloy hub.

6.1.4. Internals

The internal structural arrangement of the reactor is shown in Figure 6-3 and Drawing SK13-G-865. The entire core is mounted in the core support shield, which is supported by a conical support ring welded to the reactor vessel wall 23.8 inches below the center of the upper flow nozzles. The internals are removable either as individual components or as integral assemblies.

The fuel container assembly is confined between lower and upper grid plates approximately 90 inches apart. The fuel elements and structural internals are held down against the net upward thrust of the primary coolant flow by the main holddown spring.

The main holddown spring transmits a downward force from the vessel head to the internals and counteracts the upward hydraulic forces during operation. It also retains the internals even if the ship should capsize. The load is transferred through the upper flow baffle assembly to the core support ring in the vessel.

The orifice seal plate is bolted directly to the upper flow baffle assembly and provides a sealing surface for the 21 control rod nozzle seals. These seals are maintained by springs in the 21 control rod nozzles.

The upper flow baffle assembly, located between the orifice seal plate and the upper grid plate, consists of a series of 16 flow tubes surrounded by a vertical cylindrical chamber contained between upper and lower cover plates. There

are 18 vertical gusset plates, which support the bearing ring around the periphery. Control rod guide blocks, which run from the upper cover plate to the bottom cover plate, help position the control rods under adverse pitch-and-roll conditions.

The flow tubes direct the primary system coolant into the upper plenum of the reactor vessel and prevent crossflow. The flow tubes also prevent lateral forces against the control rod extensions when the rods are withdrawn.

The upper grid plate is a welded assembly consisting of flow tubes, various vertical baffles, and upper and lower cover plates. The outer region of the grid plate assembly acts as a turnaround manifold for coolant entering the second-pass fuel elements from the thermal shield area. The flow tubes carry the third-pass coolant directly from the fuel elements to the corresponding flow tubes of the upper flow baffle assembly.

The first and second coolant passes are separated by the main core seal formed at the perimeter of the lower plate of the grid plate assembly and the top of the inner thermal shield.

The fuel container assembly consists of 32 fuel element containers, transition pieces, a base plate, and a cylindrical thermal shield. Normally, the fuel container assembly is not removed when the reactor is refueled.

The lower flow baffle is a welded assembly consisting of flow tubes, mounted between upper and lower cover plates and surrounded by a vertical cylindrical shield. Twenty-one emergency control rod snubbers are mounted on the bottom of the lower plate.

The peripheral flow tubes direct the flow from the second-pass fuel elements into the lower plenum chamber. The center flow tubes conduct the flow from the lower plenum chamber to the third-pass fuel elements.

The emergency snubber, a combination of a spring and a hydraulic damper, absorbs the kinetic energy of a control rod if one should be dropped during loading of the rods into the reactor.

The core support shield, the center one of three thermal shields, has the dual function of protecting the vessel wall from radiation damage and supporting the entire lower flow baffle, the lower plenum chamber, and the fuel container assembly. It is suspended from and bolted to the conical support ring. A flange at the bottom supports the fuel container assembly and the lower flow baffle assembly. The lower plenum chamber also is bolted to this flange.

The lower plenum chamber consists of a circular cylinder closed on the bottom by an elliptical head. It encloses the region around the lower flow baffle assembly and the emergency control rod snubbers. The chamber turns the flow from the second pass into the third pass, and it separates the inlet coolant flow from the flow that has just left the second-pass fuel elements.

There are three thermal shields: the inner thermal shield in the fuel element container assembly, the core support shield, and the fixed or outer thermal shield permanently attached to the vessel wall. All are concentric, stainless steel cylinders.

6.1.5 Shuffled Core

The original core (Core I) was installed in the reactor in 1961. The sixteen center, or second pass, fuel elements contained UO_2 enriched to 4.2% U-235. The remaining sixteen third pass fuel elements were enriched to 4.6%.

At the end of Core I lifetime, a shuffle operation was conducted to obtain Core Ia. In this operation the four center elements were removed and replaced with four spare elements, two of 4.6% enrichment and the other two of 4.2%. The remaining 28 elements were rearranged to increase reactivity. Basically, the inside elements were moved out and the outside elements were moved in.

While the shuffle operation has provided the additional reactivity needed for 8500 Effective Full Power Hours of operation of the reactor, it did not significantly change the physical characteristics of the core. Therefore; the reactivity coefficients which are strongly controlled by these characteristics have not been changed in any significant degree.

6.2 Thermal and Hydraulic Design

6.2.1 Design Criteria

The thermal and hydraulic design criteria are:

1. Bulk boiling will not be permitted during steady state operation.
2. The local heat flux will not exceed the design value of the burnout heat flux during normal operation or during normal transient operation.

3. Local values of the fuel central temperature will not exceed the melting temperature of the fuel under the worst possible combination of manufacturing tolerances, neutron flux distribution, and fluid flow conditions during normal steady state operation or during normal transient operation.

4. All components will receive sufficient coolant flow to keep thermal stresses to a minimum.

6.2.2 Hydraulic Performance

The core flow paths and the resultant flow distribution are shown in Figure 6-4. The core and the orifice flows are based on system data; other flows are based on calculated resistances.

6.2.3 Thermal Performance

The thermal performance of the core is summarized in Table 6-2. In all calculations, the nominal power of the core is 80 MWt, and the nominal flow is 9.4×10^6 lb/hr.

Table 6-2. Thermal and Hydraulic Characteristics

<u>Parameter</u>	<u>Value</u>
Reactor thermal output, MWt	80
Design pressure, psig	2000
Operating pressure, psig	1730
Power distribution factors:	
Axial	1.79
Radial-Local	2.41
Overall product	4.31
Coolant flow rates, lb/hr:	
Primary system	9.4×10^6
Core	7.96×10^6
Bypass	1.44×10^6
Second-pass elements	7.38×10^6
Third-pass elements	6.60×10^6
Control rods	0.78×10^6
Coolant temperatures, F:	
Saturation	617
Average	508

Table 6-2. (Cont'd)

<u>Parameter</u>	<u>Value</u>	
Surface heat fluxes at rated power, Btu/hr-ft ² :		
Average	72,300	
Nominal channel *	319,000	
Hot channel **	370,000	
Reactor power at following conditions, % rated power:		
Hot channel bulk boiling at 100% flow	226	
Burnout at 100% flow	206	
Central melting at 100% flow	140	
Flow areas, ft ² :		
Thermal shield	18.72	
Each core pass	4.59	
Heat transfer areas, ft ² :		
Total	3778	
Each core pass	1889	
Temperatures at rated power, F:		
	<u>Nominal channel</u>	<u>Hot channel</u>
Surface	623	623
Fuel	3200	3700

*The nominal channel is assumed to be located in the region of maximum flux, but does not include the effect of manufacturing tolerances.

**The hot channel has the maximum flux with the accumulated effects of all manufacturing tolerances.

One of the most important factors affecting the fuel temperature is the gap between pellets and fuel rods. The thermal resistance of this gap varies because:

1. The gap thickness varies with core power.
2. The gap thermal conductivity varies with fuel burnup.

Since the fuel and cladding have different coefficients of thermal expansion and different average temperatures at a given power level, the gap size and thus the heat transfer characteristics of the fuel pins vary with reactor power.

The thermal conductivity of the gap changes with fuel burnup due to the release of fission gases to the gap. The gap is initially filled with helium, which has a thermal conductivity of approximately 0.15 Btu/hr-ft-F at the operating temperature. Low-conductivity gaseous fission products, primarily the xenons and kryptons, gradually diffuse into the gap, reducing the thermal conductivity of the gas gap and raising the fuel temperature. The diffusion rate of the fission gases from the fuel is a function of the neutron flux, the temperature and density of the fuel, and the length of time of irradiation. Fuel temperature is thus dependent on the fission gas release. Analysis of the hot channel fuel temperatures demonstrates that, in normal operation, the melting temperature of UO_2 is not exceeded.

6.2.4. Burnout

At the critical heat flux, nucleate boiling stops and film boiling begins. Exceeding the critical heat flux causes a departure from nucleate boiling (DNB). The film temperature drop increases rapidly at the onset of film boiling, and the DNB may be followed by damage to the cladding. This damage, which results from excessive temperatures, is called a burnout.

The burnout correlation used in the design calculations is the following best-fit form of the WAPD¹⁰ correlation:

$$Q''_{BO} = \frac{0.28 \times 10^6 (1 + G/10^7)^2}{(h_i/10^3)^{2.5} \exp [0.0012(X_i - X_o)/De]} \quad (6-1)$$

where Q''_{BO} = burnout heat flux, Btu/hr-ft²
 X_0 = start of heated length, ft
 X_1 = location of interest, ft
 G = flow rate, lb/hr-ft²
 h_i = coolant enthalpy at point X_1 , Btu/lb
 De = equivalent diameter of channel, ft

It is recommended that the burnout heat flux used be only 65% of the best-fit value. In addition, a safety factor of 1.2 is applied to the burnout heat flux. Thus, the design equation used is:

$$Q''_{BO} = \frac{0.152 \times 10^6 (1 + G/10^7)^2}{(h_i/10^3)^{2.5} \exp[0.0012(X_1 - X_0)/De]} \quad (6-2)$$

The burnout power is defined as the core power yielding a local heat flux equal to the burnout heat flux at some point in the core. The determination of the burnout power involves the comparison of the surface heat flux with the burnout heat flux, normally as the following ratio:

$$DNBR = \frac{Q''_{BO}}{Q''} \quad (6-3)$$

where DNBR - departure from nucleate boiling ratio
 Q'' = fuel rod surface heat flux, Bru/hr-ft²

The reactor power at which the DNBR is equal to one is called the burnout power. As long as the DNBR is greater than one, safe operation is indicated. It is noted that the difference between the design equation and the best-fit burnout equation offers a margin of safety.

The determination of the burnout power is an iterative process, which requires an assumption of a burnout power followed by a demonstration that burnout does occur. The core flow distribution is computed for the assumed power.

The hot bundle flow is then known, and the hot channel flow is found by equating pressure drops. With the known hot channel flow, the DNBR is found over the hot channel length. If the minimum DNBR in the channel is equal to one, the analysis is complete since the burnout power has been determined. If the minimum DNBR is greater than one, the assumed power is increased, and another iteration is performed. It is noted that, when the DNBR is one, there is still a margin of 1.85 before the surface heat would be equal to the best-fit burnout heat flux. As indicated in Table 6-2 above, it is expected for the present core that a DNBR greater than one is always extant when the reactor power is equal to or less than 200% of 80 MW, or 160 MW.

6.3 Nuclear Characteristics

The nuclear characteristics of the NS Savannah's core have been determined by one-, two-, and three-dimensional calculations and by measurements made at various intervals during the core life. Although the measurements generally confirm the calculations, the differences in these two methods of analysis are explained where the results show significant variations. In all cases, however, the measurements show the core design to be conservative.

The core nuclear characteristics presented herein are the results of a calculation program done in 1963 and 1964. The calculations are based on measured characteristics of the core.

To augment the extensive calculation program, the core has been subjected to a number of physics test programs. A zero-power test program was conducted at B&W's Critical Experiment Laboratory in Lynchburg, Virginia. The core excess reactivity, flux and power distribution control rod group and pattern worths, and power-peaking values for various control rod patterns were determined. In addition to the

initial physics test program, the following periodic ship-board physics tests have been conducted:

Zero-power tests at Camden, New Jersey.¹¹
500 EFPH tests at Yorktown, Virginia.¹²
1399 EFPH tests at Galveston, Texas.¹³
3078 EFPH tests at Philadelphia, Pennsylvania.¹³
4246 EFPH tests at Galveston, Texas.⁵³
7076 EFPH tests at Galveston, Texas
10174 EFPH tests at Hoboken, New Jersey
14290 EFPH tests at Hoboken, New Jersey
End of Core I life tests Hoboken, New Jersey
Core Ia initial tests at Galveston, Texas

6.3.1 Core Description

The core nuclear characteristics are summarized in Table 6-3. A midplane cross-sectional layout of the core, showing the locations of the fuel elements, control rods, thermal shields, and nuclear instrumentation, is shown in Figure 6-3.

All of the physics evaluations are based on a rated core power of 74 MWt. The fuel density used for physics calculations is 91.7% of theoretical density. This density represents the average density of the fuel as loaded in the fuel rods. The difference between the measured pellet density of 93% of theoretical density and the calculated homogenized density of 91.7% of theoretical density results from voids between adjacent pellets due to the dished pellet heads.

For nuclear calculations, the core is assumed to be a right circular cylinder. The radius of the cylinder is determined so that the cross-sectional area of the cylinder is equal to the cross-sectional area of the core. The circular cylinder is composed of homogenized unit lattice (fuel element) cells, which are defined as the square or hexagonal areas enclosed by lines drawn through the centers of control rods or water

channels surrounding the unit lattice cells. Each homogenized unit lattice cell, therefore, consists of fuel rods, moderator, a fuel element can, flow blocks, and the control rod or follower. A unit fuel rod cell is composed of a single fuel rod and its associated water and structural material.

Volume fractions and homogenized number densities are determined for a unit fuel rod cell, a third-pass homogenized fuel element, and a second-pass homogenized fuel element. Table 6-4 gives the volume fractions and number densities at cold (68F) and hot (508 F) conditions.

Table 6-3. Core Ia Nuclear Characteristics

<u>Parameter</u>	<u>Volume</u>
Initial fuel inventory, kg:	
U-235	269.5
U-238	6789.8
PU-239	13.7
Fuel enrichment, wt % U-235:	
Core average	3.81
Average thermal neutron flux at 74 MWt, n/cm ² -sec	7.2 x 10 ¹²
Volume fractions:	
Water	0.567
Control rods	0.041
Fuel	0.247
Stainless steel	0.145
Metal/water ratio	0.76

**Table 6-4. Volume Fractions and Number Densities,
Unit Fuel Rod Cell**

<u>Volume Fraction</u>		
<u>Material</u>	<u>Volume, in³</u>	<u>Volume Fraction</u>
UO ₂	9.3409	0.3220
Cladding	3.3745	.1163
Ferrules	0.1836	.0063
Helium gas	0.2436	.0084
H ₂ O	<u>15.8690</u>	<u>0.5470</u>
	29.0116	1.0000

<u>NUMBER DENSITY</u>		
<u>Material or Isotope</u>	<u>Number density at 68F atoms/barn - cm</u>	<u>Number denisty at 508F atoms/barn - cm</u>
U-235	0.00027696	0.00027696
U-238	0.00000986	0.00000986
Pu-239	0.000013643	0.000013643
Pu-240	0.000001238	0.000001238
Pu-241	0.000000243	0.000000243
Pu-242	0.000000010	0.000000010
Stainless steel	0.010593	0.010593
H	0.036530	0.036530
O	0.032655	0.032655

6.3.2 Reactivity Coefficients

Four inherent reactivity effects characterize the NS Savannah reactor during operation. These effects are associated with changes in fuel temperature, moderator temperature, system pressure and moderator void content. The reactivity coefficients corresponding to these changes arise from the following phenomena:

1. Doppler coefficient from changes in resonance absorption due to the Doppler broadening of neutron capture resonances in U-238 as fuel temperature changes.

2. Temperature coefficient from changes in absorption, resonance escape, leakage, and fast fission effect due to changes in water density, effective cross sections as a result of a change in the neutron temperature, and effective control rod worth due to beta particle emission.

3. Pressure coefficient from changes in absorption, resonance escape, leakage, and fast fission effect due to a change in water density.

4. Void coefficient from changes in absorption, resonance escape, leakage, and fast fission effect due to a change in water density.

These reactivity coefficients have been calculated as a function of core lifetime using the one-dimensional model. The coefficients (except the void coefficient) have also been measured at periodic intervals during the core life. The measured and calculated results are in very good agreement and show large negative coefficients for the temperature, Doppler, and void effects. These negative coefficients ensure stability and safe reactor operation. The pressure coefficient is slightly positive. During reactor transients this coefficient reduces the effectiveness of the temperature coefficient by a small (nearly negligible) amount. The

operating coefficient is also considered and discussed because of its importance to ship maneuverability using manual control.

6.3.2.1. Doppler Coefficient

The Doppler coefficient of reactivity is the reactivity change due to the Doppler broadening effect in the fertile U-238. The reactivity effect is negative and in two-group theory is accounted for in the resonance escape probability.

The power Doppler coefficient is defined as the change in core reactivity due to a change in core power. The power coefficient defined in this manner is calculated to increase during burnup due to an increase in the average fuel temperature during power operation. The increase in fuel temperature is due to the decrease of the thermal conductivity of the pellet gap gas (between the pellet and cladding wall of the fuel rods) by dilution of the highly conductive helium gas with the fission product gases, krypton and xenon. However, a positive effect (lowering of the fuel temperature) occurs during burnup due to fuel pellet cracking, which decreases the effective gap thickness between the pellet and the cladding. The calculational model was based on the assumptions that no fuel cracking occurs, that 20% of the fission gases reach the gap, and that the reactivity deficit depends on the average fuel temperature with a weighting factor of unity. The calculation results for Core I are presented in Table 6-5, which gives the calculated reactivity deficit in terms of both absolute and dollar reactivity units for various time steps in core life.

Table 6-5. Calculated Core I Doppler Coefficient of Reactivity and Total Reactivity Deficit

Time step, EFPH at 74 MWt	Doppler reactivity deficit ()	Doppler coefficient, / F	Power Doppler coefficient	
			/MWt	/MWt
0	0.0030	-0.93×10^{-5}	-0.41×10^{-4}	-0.58
500	.0038	$-.97 \times 10^{-5}$	$-.51 \times 10^{-4}$	-0.73
1,399	.0048	$-.94 \times 10^{-5}$	$-.65 \times 10^{-4}$	-0.93
2,500	.0060	$-.95 \times 10^{-5}$	-0.81×10^{-4}	-1.17
5,000	.0075	$-.95 \times 10^{-5}$	-1.01×10^{-4}	-1.47
10,000	.0092	-0.97×10^{-5}	-1.24×10^{-4}	-1.85
16,000	0.0108	-1.00×10^{-5}	-1.35×10^{-4}	-2.09

Table 6-6 has measurements of the Core I power Doppler coefficient. These measurements show that the coefficient is independent of core power.

Table 6-6. Measured Core I Power Doppler Coefficient From Uncontrolled Transients at 2335 EFPH Hot, Partial Xenon Conditions

Test number	Reactor power change, P, MWt	Average temp change, T, F	Doppler coefficient, MWt
1	15.66	6.00	-1.03
2	15.90	7.00	-1.19
3	15.50	5.25	-0.92
4	16.20	7.00	-1.17
5	10.85	5.25	-1.30
6	12.28	4.74	-1.04
7	12.33	6.75	-1.48

The results of the measurements and the calculation of the Doppler coefficient are given in Figure 6-5 as a function of core lifetime. The measured results indicate that the coefficient has remained essentially constant. This trend is expected to hold throughout lifetime of Core I and Core Ia.

6.3.2.2 Moderator Temperature Coefficient

The moderator temperature coefficient is a slow-acting coefficient when compared to the Doppler coefficient.

The time lag results from the relatively long heat transfer time constant of the fuel. The mean thermal neutron temperature, which affects the coefficient through the cross sections of the various core materials, also suffers from this time lag because the effective neutron temperature is about equal to the moderator temperature.

The presence of Pu-239 and fission products tends to reduce the coefficient with burnup. Because of the large Pu-239 resonance at 0.3 ev (within the thermal energy cutoff at 0.4 ev), the presence of Pu-239 decreases the coefficient because, as the temperature of the moderator rises, the mean energy of the neutron spectrum also rises. However, the ratio of the capture to fission cross sections for Pu-239 also rises, thus helping to offset this effect.

Determination of the moderator temperature coefficient as a function of core burnup required two calculations. The first calculation considered the effects of moderator density, moderator temperature, fission products, and plutonium buildup and cross sections assuming no control rods in the core. The second calculation considered the effect of increasing control rod worth with increasing moderator temperature.

The measured and calculated values for the Core I moderator temperature coefficient at hot, operating conditions are shown in Figure 6-6 as a function of core burnup. The calculated and measured values for the moderator temperature coefficient over the operation temperature range at initial and end-of-life conditions for Core I are given in Figure 6-7. The moderator temperature coefficient is measured at various stable core temperatures during heatup of the primary system. The measurements include the effect of control rods, and therefore at each stable temperature plateau the total moderator coefficient is measured.

The conclusion from the various calculations and measurements is that the moderator temperature coefficient is a large negative coefficient at hot, operating conditions. It is initially equal to about 2.8 cents/F and decreases to about 2.0 cents/F at the end of core life. The decrease is due to a smaller control rod effect and the buildup of plutonium with core burnup.

6.3.2.3 Pressure Coefficient

With changes in primary system pressure, the density of the moderator changes, giving rise to changes in reactivity. This effect, the pressure coefficient of reactivity, is positive and during plant transients tends to reduce the effectiveness of the moderator temperature coefficient. Measurements of the pressure coefficient are taken at constant moderator temperatures by simply increasing and decreasing the primary system pressure. Calculations were made using a technique similar to that used for the moderator coefficient. The calculated and measured values of the pressure coefficient at hot, zero-power conditions are given in Figure 6-8 as a function of Core I burnup.

6.3.2.4 Void Coefficient

One of the basic assumptions in the original design of the core was that bulk or local boiling would not be permitted in normal operation. Thermal calculations indicate that a slight amount of local boiling does occur in the hot channels at the full rated power of 80 MWt. At the original design power (69 MWt) no voids are present. The calculational technique was identical to that for the moderator temperature coefficient calculation. The calculational results are given in Figure 6-9 at hot operating conditions as a function of Core I burnup. Measurement of the void coefficient is not feasible because significant voids are not formed at permissible operating power.

6.3.2.5 Operating Coefficient

The operating coefficient is defined as the change in reactor power per degree of temperature change of the coolant. It is equal to the moderator temperature coefficient divided by the power Doppler coefficient.

During normal operation, as the power level increases due to rod withdrawal, these two reactivity coefficients (moderator temperature and power Doppler) combine to limit the reactor power. During uncontrolled transients, however, these two coefficients act against each other. Thus, if the ratio of the temperature coefficient to the Doppler coefficient is large, the change in the average coolant (moderator) temperature is fairly small for significant load changes.

The operating coefficient is determined from an uncontrolled transient by measuring the change in the primary system average temperature associated with a secondary steam load change without compensating control rod motion. The observed ease of manual high value of the operating coefficient. At 2335 EFPH the measured operating coefficient was about 2.4 MWt/oF. This means that no immediate control rod motion is needed for load changes of up to about 20 MWt. Secondly, it has been observed that, after an uncontrolled load change, about 3 minutes is required for the plant (including primary system temperature) to attain equilibrium conditions. Therefore, during normal operation when the primary system temperature is held at 508 F, this time lag of 3 minutes allows the reactor operator more than ample time to either insert or withdraw the required amount of reactivity.

Table 6-7 gives the measured results of the Core I operating coefficient from the 1420, 2335, and 4246 EFPH tests.¹³

Table 6-7. Measured Operating Coefficients
Hot, Partial Xenon Conditions

<u>Run number</u>	<u>Reactor power, MWt</u>			<u>Reactor temp, F</u>		<u>Temp change, F</u>	<u>Operating coefficient, MWt/F</u>
	<u>Initial</u>	<u>Final</u>	<u>Change</u>	<u>Initial</u>	<u>Final</u>		
<u>1420 EFPH results</u>							
1	20.60	13.32	7.28	506.39	508.92	2.53	2.88
2	13.32	29.58	16.26	507.90	500.50	7.40	2.20
3	38.18	24.90	13.28	506.62	510.81	4.19	3.17
4	25.35	41.35	16.00	509.80	503.20	6.60	2.42
5	49.21	38.66	10.55	507.15	510.80	3.65	2.89
6	38.66	58.95	20.29	510.80	502.70	8.10	<u>2.50</u>
Average							2.68
<u>2335 EFPH results</u>							
1	60.13	44.47	15.66	507.08	513.08	6.00	2.61
2	44.17	60.37	15.90	513.08	506.08	7.00	2.27
3	48.99	33.49	15.50	506.58	511.83	5.25	2.95
4	33.49	49.69	16.20	511.83	504.83	7.00	2.31
5	28.81	39.66	10.85	509.33	504.08	5.25	2.07
6	28.92	16.64	12.28	506.58	511.33	4.75	2.59
7	16.64	28.97	12.33	511.33	504.58	6.75	<u>1.83</u>
Average							2.38
<u>4246 EFPH results</u>							
1	32.17	16.22	15.95	507.75	510.75	3.00	5.32
2	16.22	31.91	15.69	510.75	506.00	4.75	3.30
3	40.98	25.22	15.76	507.00	511.50	4.50	3.50
4	25.22	41.06	15.84	511.50	506.25	5.25	3.02
5	51.66	38.42	13.24	507.00	511.25	4.25	3.12
6	38.42	51.74	13.32	511.25	507.25	4.00	3.33
7	64.92	49.57	15.35	507.75	512.00	4.25	3.61
8	49.57	62.95	13.38	512.00	508.00	4.00	<u>3.35</u>
Average							3.57

The measured and calculated operating coefficient results are plotted in Figure 6-10 as a function of core burnup. The calculated operating coefficient is only 1.3 MWt/°F at the end of core life. This low calculated value is due to the increase in the Doppler coefficient. Based on the measured value of the power coefficient at 3078 EFPH, the end-of-life operating coefficient should be approximately 2.2 MWt/°F.

6.4 Shipboard Physics Test Program

6.4.1 Program Objectives

The operational program of the NS Savannah includes periodic measurements of core nuclear characteristics throughout the core lifetime. The purpose of these tests is to check the predicted nuclear characteristics and to ensure the continued safety of core operation.

During each of the tests, normal reactor startup and heatup operations are modified and extended to measure the reactor and plant operating characteristics. In general, each testing period consists of zero- and low-power dockside tests and additional tests at various reactor power levels at sea. The dockside tests are made at various primary system nominal temperature plateaus. At each of the temperature levels, the critical control rod positions are determined for different control rod patterns, the temperature coefficient is measured, and the calibration of nuclear instrumentation channel 6 is performed. During heatup between the temperature plateaus, a control rod group (either the C, B, X, or A group) is calibrated. Further tests, including power Doppler, operating coefficient, and transient tests, are conducted at base-load and sea trial operations. The sequence of events for the 1399 and 3078 EFPH tests is shown in Table 6-8.

Table 6-8 . Sequence of the 1399 and 3078 EFPH
Physics Tests

1399 EFPH physics tests

Primary system temperature at 205, 250, 350, 425, 475, and 508 F:

1. Reactor startup at 205 F.
2. Critical control rod positions:
 - a. A-group banked sequence.
 - b. Out-in sequence.
 - c. In-out sequence.
 - d. Proposed Marvel-Schebler sequence.
3. Temperature coefficient of reactivity.
4. Nuclear instrumentation calibration.

Primary system temperature at 508 F:

1. Calibration of A-group control rods.
2. Pressure coefficient of reactivity.
3. Power Doppler coefficient of reactivity.

Sea trial operations:

1. Measure operating coefficient at 22, 37, 52, and 66.5 MWt.
2. Calibrate nuclear instrumentation channels 8, 9, 10, and 6 at various stable power levels.

3078 EFPH physics tests

Reactor startup and nuclear instrumentation overlap at 250 F.

Heat up to 300 F, calibrate B-group control rods.

Primary system temperature at 300, 450, 508 F:

1. Critical control rod positions:
 - a. Out-in sequence.

Table 6-8. (Cont'd)

- b. In-out sequence.
- c. A-group banked sequence.
2. Temperature coefficient of reactivity.
3. Nuclear instrumentation calibration.
4. Calibrate B-group rods during heatup.

Primary system temperature at 508 F:

1. Nuclear instrumentation overlap.
2. Power Doppler coefficient of reactivity.

Sea trial operations:

1. Measure operating coefficient at 18.5, 29.6, 40.7, and 52 Mwt.
2. Calibrate nuclear instrumentation channels 8, 9, 10, and 6 at various stable power levels.

The following are special reactor plant operating conditions that apply to the dockside portions of the test program:

1. Initial criticality is specified at a primary system temperature of 250 to 300 F (205 F for the 1399 EFPH tests). Precritical checkouts are performed as normally required. Primary system pressure is maintained at its normal value with no pressurizer spray below 350 F.
2. Weak source startups are carried out if the Po-Be and the photoneutron sources have decayed to less than 1.5 counts per second (minimum count rate interlock not energized).
3. Shoreside power is required to provide electrical power to various ship power demands so that the diesel generators can be used to supply the electrical power necessary to operate four primary pumps at full speed.

4. Deviations from the normal control rod withdrawal sequence are specified throughout the test program.
5. The steam generators are secured for all dockside tests except for the low-power Doppler reactivity coefficient measurements.
6. Letdown flow rate and the control rod buffer seal primary system pressure differential are varied within plant operating standard limits for nuclear instrumentation calibrations and to maintain constant primary system temperatures when required.
7. Control rod positions for all reactivity measurements are established by final downward motion of the rods.
8. Constant primary system temperature and pressure conditions required for doubling-time measurements and nuclear instrumentation calibrations are obtained by balancing the letdown flow rate and the primary system heat losses against the primary system pump heat, pressurizer heat, and (when specified) reactor heat inputs. The most stable plant conditions are obtained when the letdown flow rate is equal to the makeup flow rate as evidenced by a constant pressurizer level.

6.4.2 Nuclear Instrumentation Calibration

6.4.2.1 Low-Power Range

At the low-power range (watts to 1.5 MWt) calibration of nuclear instrumentation channel 6 is possible because an accurate heat balance can be determined. The low-power calibration is accomplished by establishing stable plant conditions at various low-power reactor inputs. These heat inputs at each temperature vary from essentially zero to approximately two megawatts. With zero reactor input, stable plant conditions are maintained by balancing the pump heat

input and pressurizer heater heat input (if spray conditions exist) against normal primary system heat losses and letdown flow heat losses. Reactor heat inputs are necessary when the number and speed of primary system pumps are reduced and the letdown flow rate is increased to the maximum value. Calibration of channel 6 is then performed by calculating the reactor heat input from a heat balance at each of the four stable plant conditions of the test. The heat balance results are directly compared to the observed channel 6 reading from the micromicroammeter.

6.4.2.2. Operating Power Range

Experience has shown that an adequately accurate measurement of reactor power, at power levels of 40% of full power or greater, may be obtained from a heat balance based on the installed nonnuclear instrumentation readings under stable operating conditions. Therefore, to perform the calibration of the power range nuclear instrumentation channels, an initial reactor operating period at a reasonably high power level is required to provide stabilized thermal plant conditions and an accurate heat balance.

To perform the calibration, two thermal measurements of reactor power are made at a 1-hour interval and compared to the percentage of full power displays from channels 8, 9, and 10. If the indications do not fall within ± 4 or -1% of the measured power, the power range amplifier gain controls are adjusted accordingly. To verify the adjustments, two additional measurements of reactor power at a 1-hour interval are required. If reasonable results are not obtained, the calibration is repeated.

6.4.3. Reactivity Coefficients

6.4.3.1. Isothermal Temperature Coefficient

The isothermal temperature coefficient of reactivity is measured at each of the temperature plateaus during the test program. The present normal method, using the A-group banked control rod pattern, involves measurement of the excess reactivity associated with four positions of the X-rod at two slightly different core temperatures. For each X-rod withdrawal position, the change in reactivity per change in temperature is computed from the difference in doubling times between the two different core temperatures.

The E-group rods are used to terminate the rise in reactor power after the completion of each set of doubling time measurements. As the reactor power is decreasing due to E-group rod insertion, the X-rod is moved to the next measurement position; the core is then brought to nearly exact critical conditions by E-group rod manipulation, and finally the E-group rods are fully withdrawn to obtain the next doubling time measurement.

6.4.3.2. Doppler Coefficient

The Doppler coefficient of reactivity is determined by a combination of two measurements. At the low-power range the coefficient is measured directly, but at the higher power ranges it is determined indirectly from the operating coefficient measurement.

Direct measurement of the Doppler reactivity deficit with rising power (increasing fuel temperature is possible at the low-power range by comparing two stable plant conditions. At zero reactor power the plant is stabilized by matching the pump heat against primary system heat losses and letdown heat losses. The transition between zero- and low-power stable plant conditions is achieved by the following

sequence:

1. Add reactivity by withdrawing the X-rod a small distance.
2. Determine the added reactivity by a doubling time measurement of the stable rising reactor period.
3. The reactor power is allowed to continue rising into the low-power range with no further control rod motion.
4. When the primary system average temperature begins to rise, steam is drawn from the steam generators.
5. The secondary steam load is then adjusted to return the plant to stable conditions and lower the average primary system temperature to the initial stable value.
6. The power coefficient is then found by dividing the initial added reactivity by the resulting power rise. This procedure is followed for three reactivity additions of approximately 5, 10, and 15 cents. Since the nonnuclear instrumentation cannot accurately measure low steam flow, the output from nuclear instrumentation channel 6, which has been previously calibrated, is used to determine the actual reactor power level. This method can be used for power levels of about 25% of full power during the transient load matching operation, but under stable conditions, is limited to the steam load that can be dissipated, excluding steam dumps and the main engine. At operating power levels, the Doppler coefficient is not measured directly. The Doppler coefficient is obtained by dividing out temperature coefficient from the measured operating coefficient.

6.4.3.3. Pressure Coefficient

Measurement of the pressure coefficient of reactivity is very similar to the determination of the temperature coefficient. The excess reactivity from four different X-rod withdrawal positions is measured at two different primary system pressures. The procedure is as follows:

1. Establish stable critical conditions with the primary system temperature at 508 F and the primary system pressure equal to 1835 psig.
2. Withdraw the X-rod a small increment to add about 8 cents of reactivity.
3. Measure the doubling time, and after consistent data are obtained, terminate the power rise with the outside of control rod group E.
4. Repeat steps 2 and 3 for reactivity additions of approximately 12 and 16 cents.
5. With X-rod at the position of the 16-cent reactivity addition, terminate the power rise with the E rods, and establish new stable primary system conditions. Keep the temperature constant at 508 F, but lower the pressure to 1635 psig.
6. Repeat steps 2, 3, and 4 in the reverse manner for this low pressure of 1635 psig.

The pressure coefficient of reactivity is then equal to the change in reactivity divided by the change in pressure.

6.4.3.4. Operating Coefficient

During power operation, the amount of self-regulation or the magnitude of allowable uncontrolled load changes is dictated by the operating coefficient and the sizing of various reactor components. The operating coefficient is equal to the temperature coefficient or reactivity divided by the power Doppler coefficient of reactivity and thus has units of megawatts per degree Fahrenheit.

Measurement of the operating coefficient is accomplished by several uncontrolled load changes at various reactor power levels. The procedure is as follows:

1. Establish and maintain stable power at least 1/2 hour. Keep the average primary coolant temperature at 508 F and the pressurizer level at about 30 inches.
2. Complete the heat balance. Do not move any rods before step 9 except in an emergency.
3. Reduce the steam load in about 10 seconds and allow the plant to stabilize.
4. Complete a heat balance (wait 5 to 10 minutes before recording data).
5. Maintain stable conditions for at least 1/2 hour. Hold the primary system coolant average temperature at about 512 F and the pressurizer level at about 35 inches.
6. Repeat recording of heat balance data.
7. Increase the steam load in about 10 seconds and allow the plant to stabilize.

8. Complete the heat balance data, maintaining the primary system coolant average temperature at 504 F and the pressurizer level at approximately 25 inches.

9. Restore the plant to normal operating conditions.

10. Measure the operating coefficient at different initial power levels by repeating steps 1 through 9. The values used normally vary from 30 to 80% of full power. The following limitations on various plant parameters are specified under current operating philosophy:

1. Steam drum pressure cannot exceed 740 psig.
2. Primary system pressure is kept within the range of 1650 to 1850 psig.
3. Primary system outlet temperature should not exceed 527 F.
4. Pressurizer level should be kept between 15 and 40 inches.

6.4.4. Control Rods

6.4.4.1. Critical Positions

Critical control rod positions are determined at each temperature level during the physics test programs for various withdrawal sequences. The sequences measured to date are designated the A-group banked, out-in, in-out, and the group overlap withdrawal sequences.

The control rods or rod groups involved in switching from one control rod pattern to another are determined by the actual existing pattern and the pattern desired. Normally, the insertion sequence of the initial pattern and the

withdrawal sequence of the final pattern are used during the switching operation. The switching or rod-swapping operation is accomplished by the insertion and withdrawal of small reactivity increments so that a zigzag-appearing recording of reactor flux level is obtained at a fairly constant average power level. The rod-swapping operation can be done fairly quickly due to the fast response of nuclear instrumentation channel 6 for small reactivity changes.

A-Group Banked Withdrawal Sequence

The A-group banked control rod withdrawal sequence, which until recently was the normal operating pattern, is a modified out-in sequence as follows: the A-group is first withdrawn 25.5 inches, followed by withdrawal of the E, D, C, B, and X rod groups as necessary. During maneuvering or during power changes, the A-group is used to control the reactivity changes caused by the power Doppler effect. Xenon shimming and burnup reactivity effects are compensated by the outside group or groups.

Out-In Withdrawal Sequence

For the out-in pattern, criticality is achieved by withdrawing the control rods in groups as follows: E, D, C, B, A, and X, i.e., from the outside to the inside. During operation, reactivity is added by this sequence and reduced by the reverse X, A, B, C, D, and E sequence. At any given time, no more than one rod group is operated and partially withdrawn. Because of pattern simplicity, critical out-in control rod positions are obtained to aid in evaluating core reactivity.

In-Out Withdrawal Sequence

The in-out control rod sequence is used to determine a subcritical margin in terms of an integral number of central control rods. This pattern involves the withdrawal

of individual rods as follows: S, A-1, A-2, A-3, A-4, B-1, B-2, etc. The subcritical margin is determined by the number of fully withdrawn control rods at critically for each temperature plateau.

Group Overlap Sequence

The group overlap sequence is a modified out-in withdrawal sequence. The feature of this sequence is that more than one group is partially withdrawn at one time. The sequence has been adopted as the normal withdrawal sequence (using a simulation technique) for the present control system. The detailed withdrawal sequence and method of simulation are presented in section 10.4.

6.4.4.2. Calibration

The control rod groups are calibrated by the temperature shim method. This method determines the incremental rod worth associated with each small change in moderator temperature. The change in reactivity corresponding to the change in control rod group position is equal to the product of the temperature coefficient and the change in moderator temperature.

Temperature shim calibration is performed during normal plant heatup. As the primary system temperature rises, the reactor loses reactivity and becomes slightly subcritical (displayed by the channel 7 linear power recorder). To compensate for this loss in reactivity, the rod group being calibrated is withdrawn several inches to add reactivity to the reactor. After this reactivity addition, the reactor becomes slightly supercritical, and the power increases until the resulting temperature increase overrides the reactivity addition. At the time the reactor power reaches its maximum value, the reactor becomes just critical. Average reactor temperature is then recorded at the just critical condition. This procedure

is followed until the rod group is completely calibrated or until the primary system has reached the normal operating temperature of 508 F. During each increment of rod group withdrawal, the reactor power varies from about one to two megawatts.

6.4.5. Transient Tests

The objective of power plant transient tests is to determine the response of the plant to load changes and load losses that may be expected under normal and extreme conditions. Specific tests which have been performed are:

1. Load changes with no reactor control.
2. Load changes with manual reactor control.
3. Loss of load from various trip actions.
4. Scram at full power.

Special recording of the important plant parameters is necessary to provide a record of each parameter value throughout the transient. Initially, a multichannel optical galvanometer displayed each of the important plant parameters on chart paper using ink pens.

The initial acceptance trial transient tests were quite lengthy and involved to prove the response of the plant to various controlled and uncontrolled transients. Recent transient tests were conducted during the 1964 sea trials. These tests concentrated on uncontrolled load changes in order to detect changes, if any, in the plant response to transients. Uncontrolled transients also provided excellent data for comparison to and improvement of analog results and models.

6.4.6. Xenon Buildup to Equilibrium

Xenon buildup to equilibrium conditions is measured by observing the changes in critical rod positions. The

measurement technique is to establish a steady state power level (if sea conditions warrant) and hold this power level for 50 hours. For best results, the high steady state power level should be established as soon as possible after startup. Further, the hot, zero-power, clean critical rod positions must be known prior to the steady state operation period. This requires a shutdown period of 48 hours prior to the experiment.

Analysis of the data requires subtracting out the Doppler lumped fission product buildup, fuel burnout, and possibly samarium buildup (if the measurement is made early in core life) reactivity deficits from the total deficit measured.

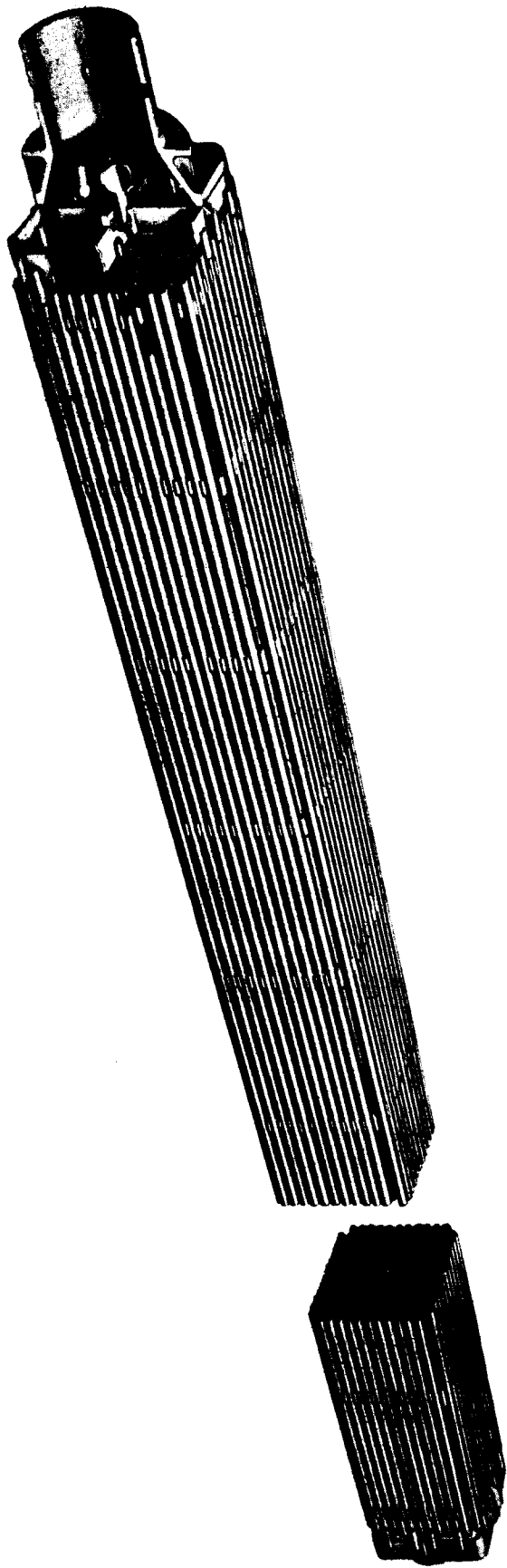


Figure 6-1. Fuel Element

Figure 6-2. Fuel Tube

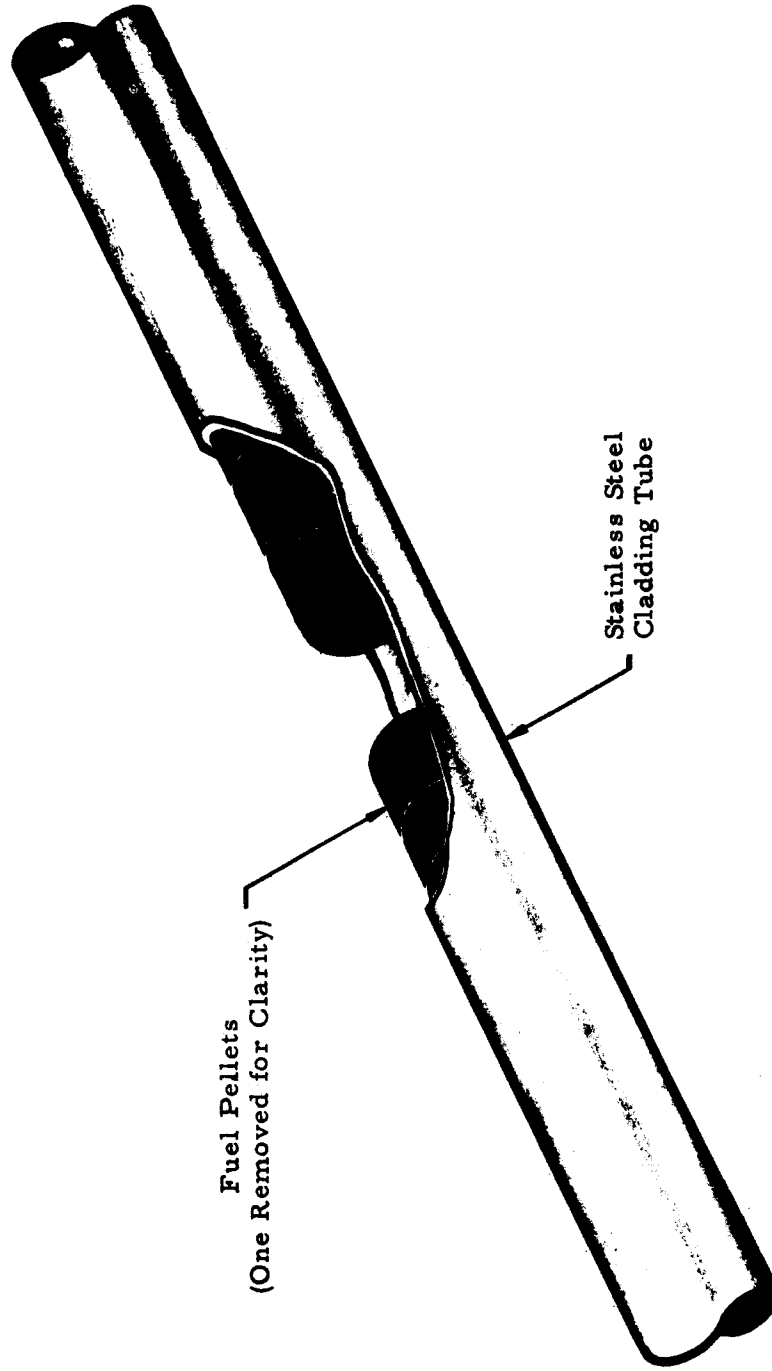


Figure 6-3. Cross Section of Core

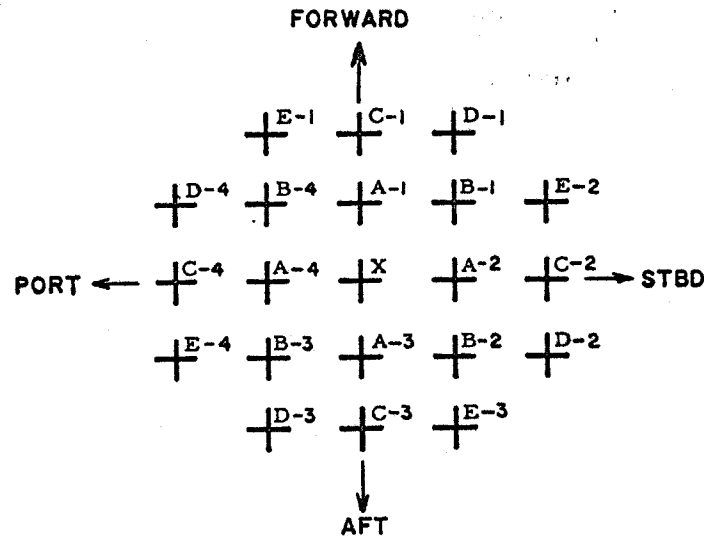
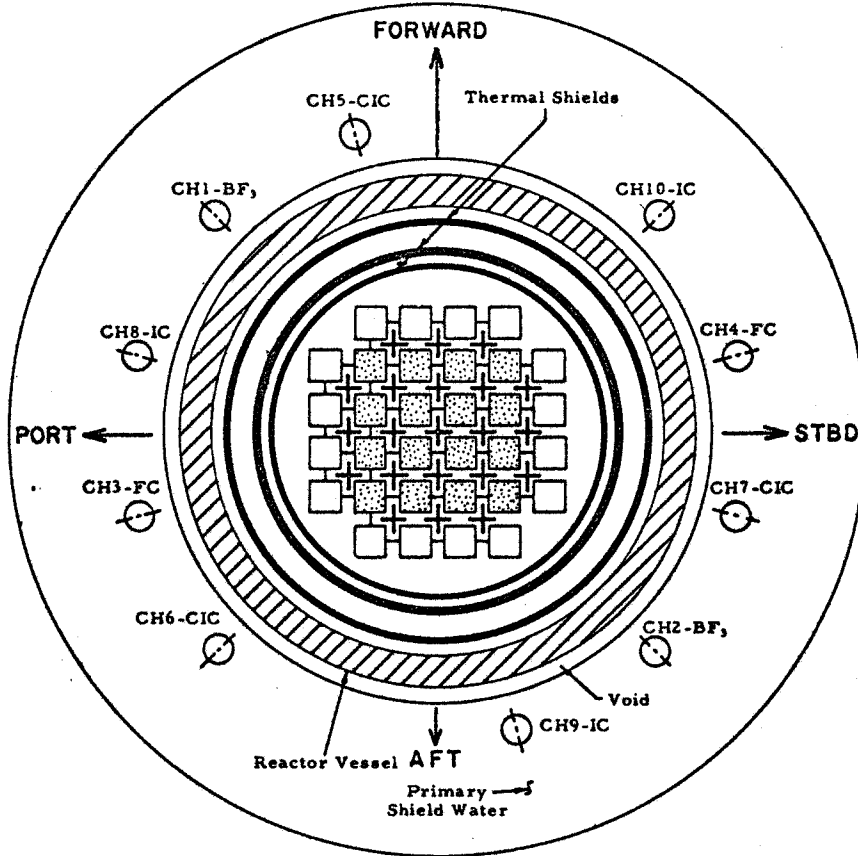


Figure 6-4. Core Flow Distribution (Design)

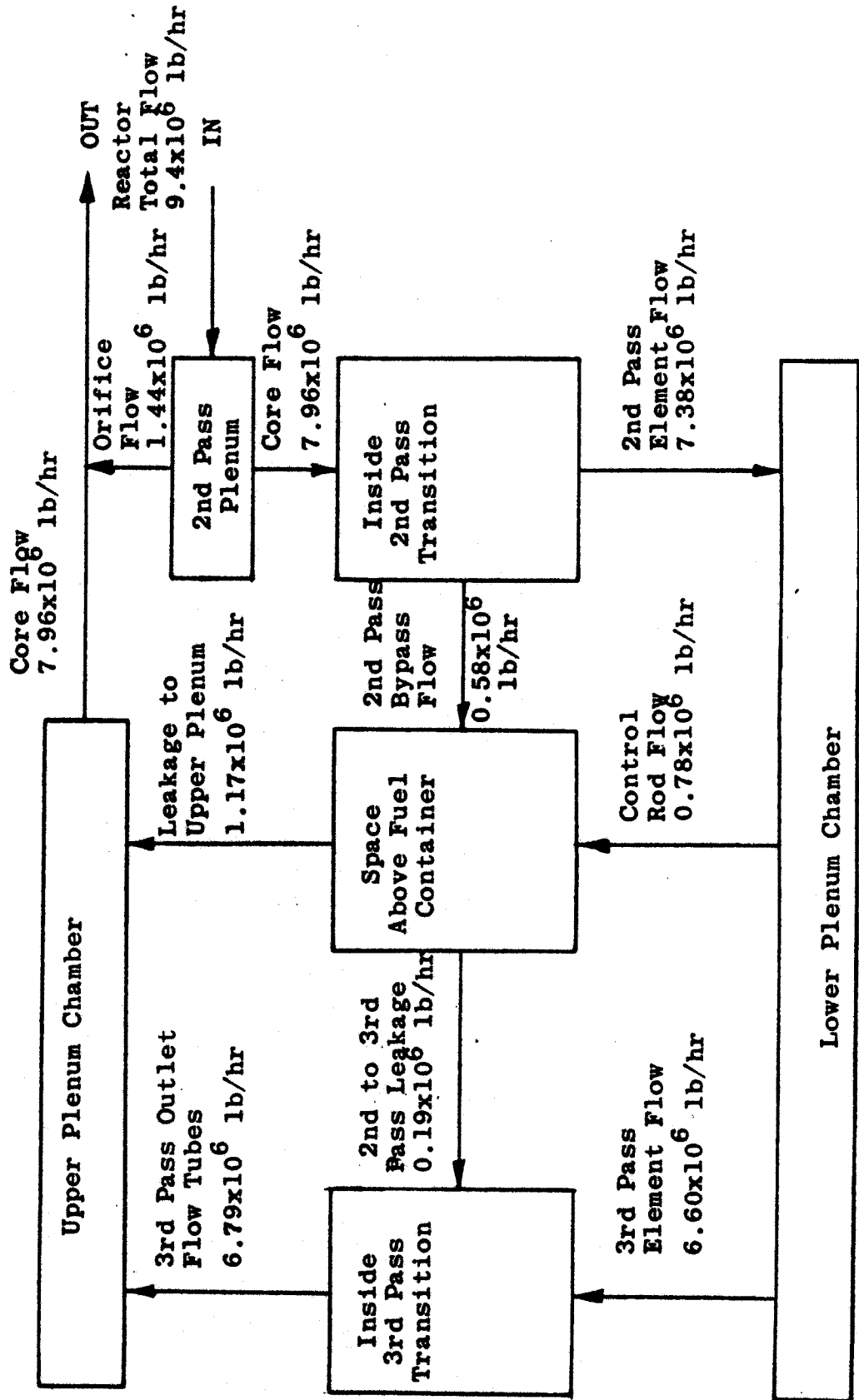
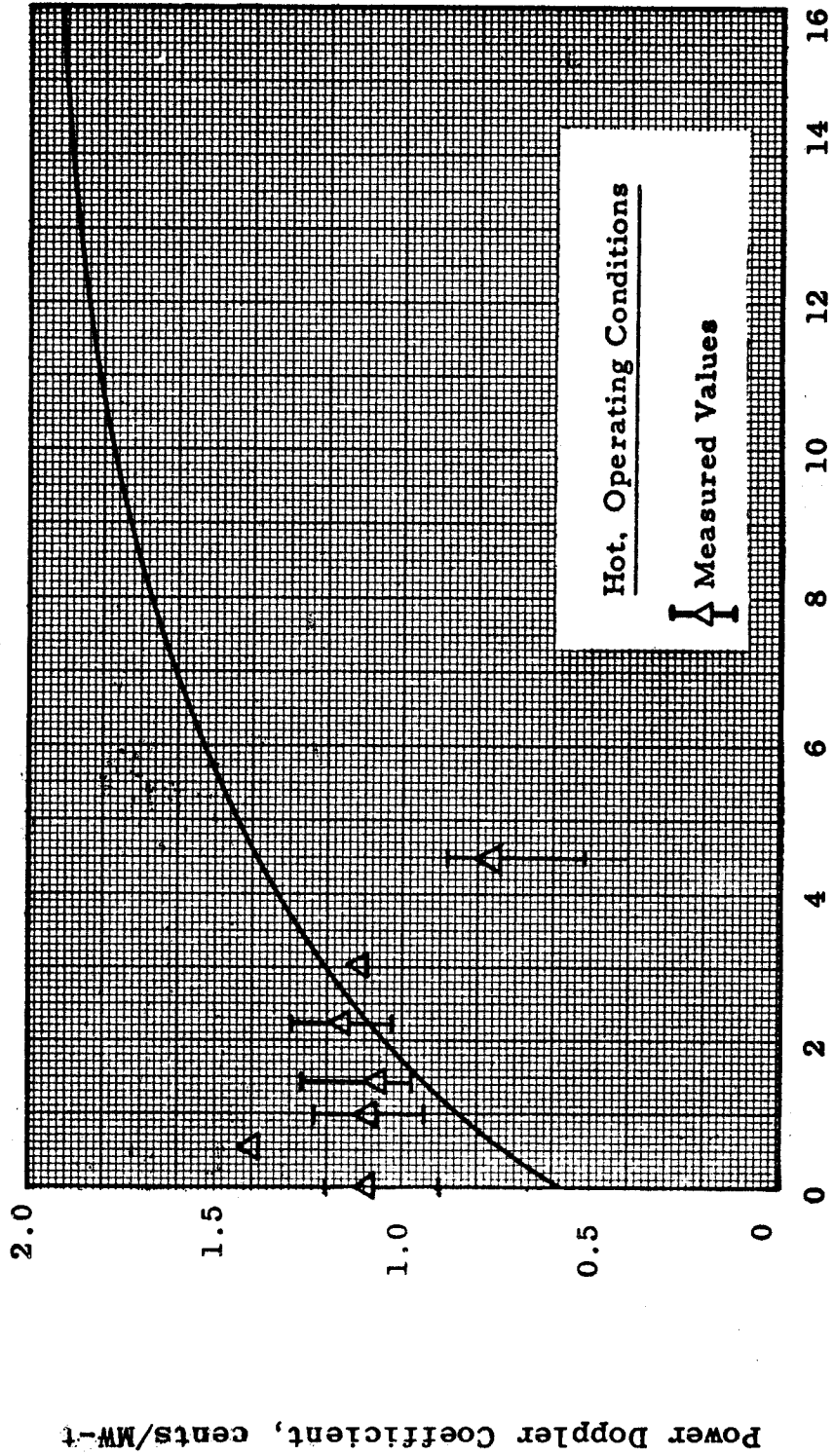


Figure 6-5. Variation of Power Doppler Coefficient
With Burnup for Core I



Core Burnup, EFPH X 10⁻³

(

(

(

Figure 6-6. Moderator Temperature Coefficient Variation
With Burnup for Core I

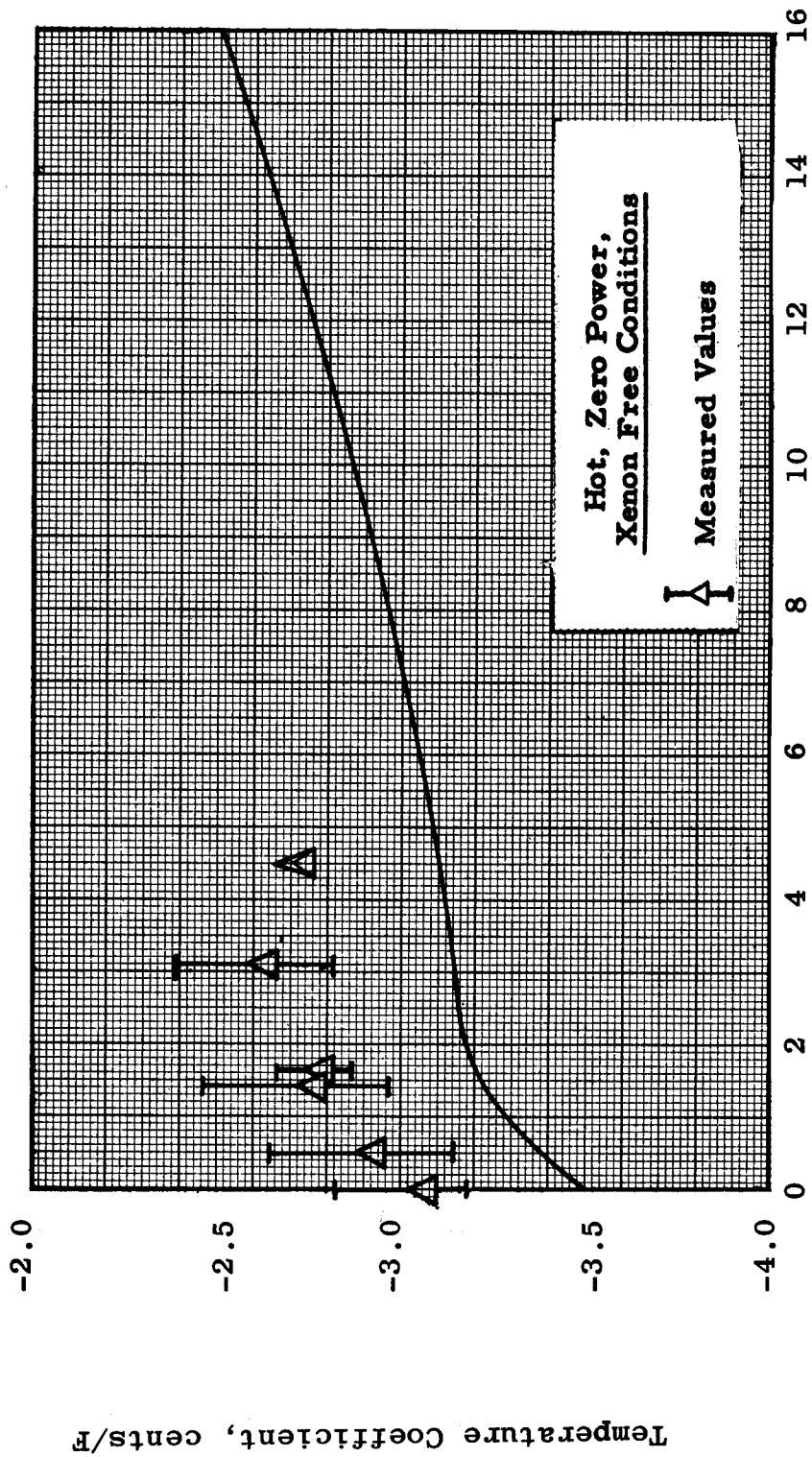
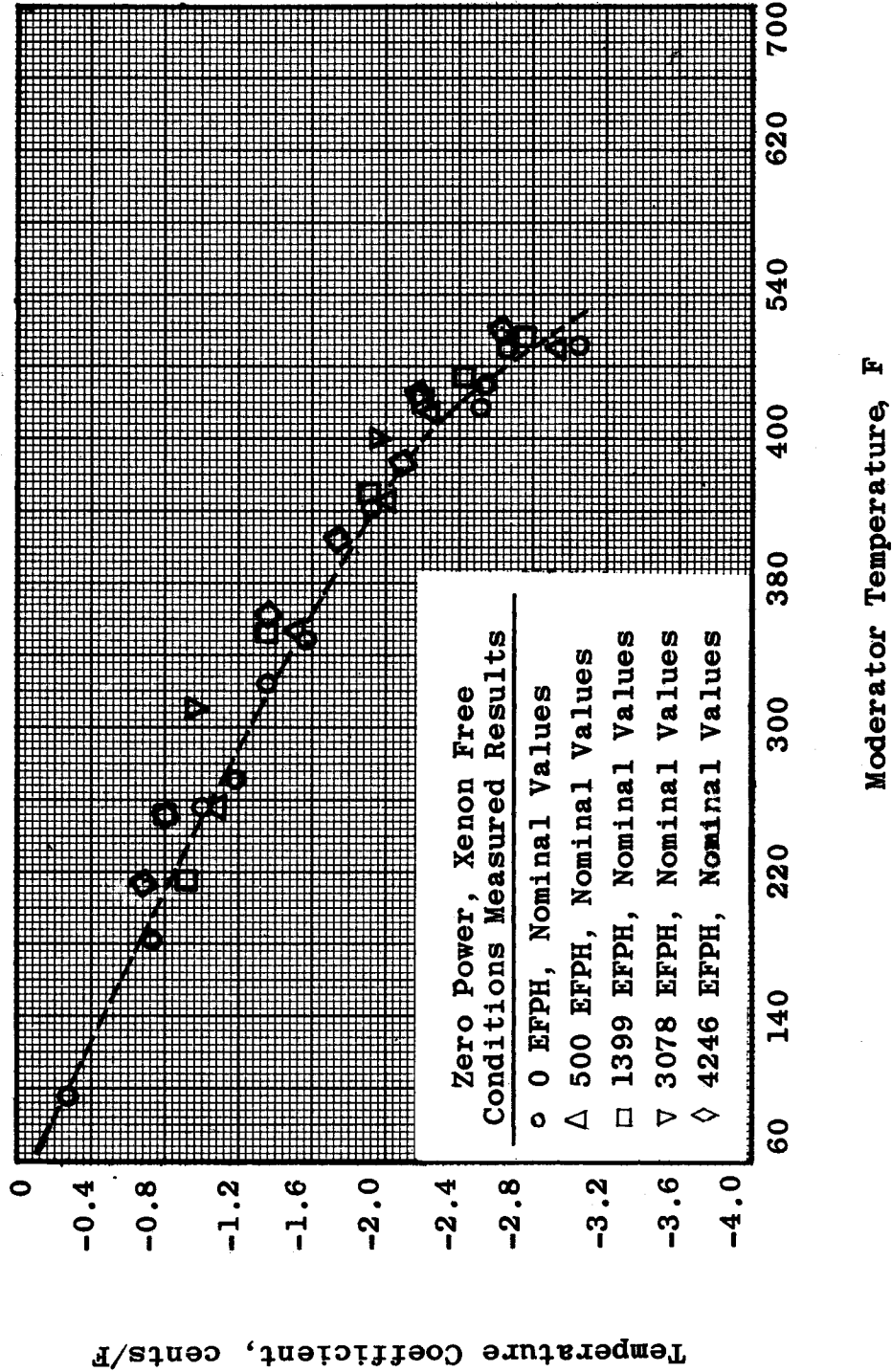


Figure 6-7. Moderator Temperature Coefficient Variations
With Moderator Temperature



Moderator Temperature, F

Figure 6-8. Pressure Coefficient vs Burnup for Core I

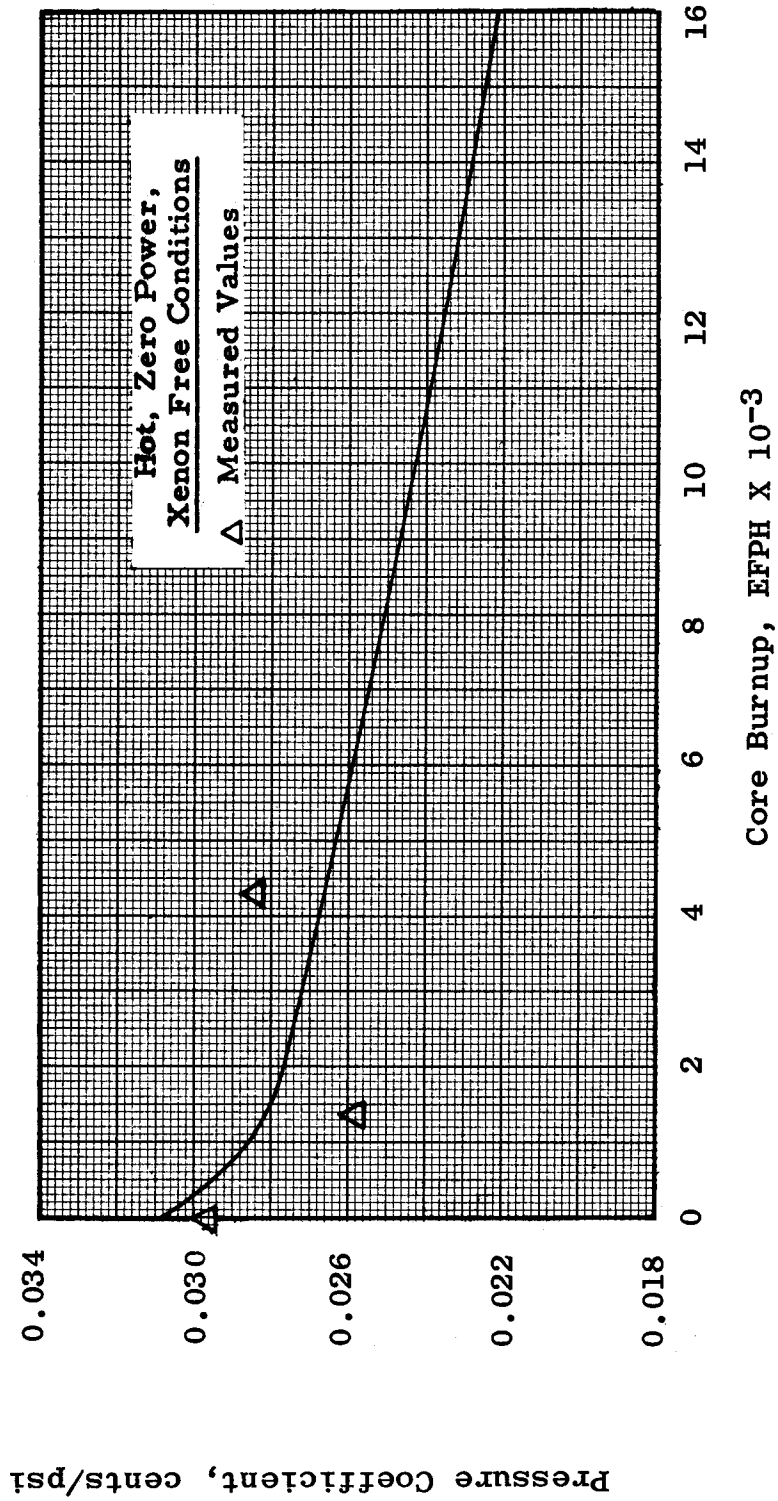


Figure 6-9. Void Coefficient Variation With Burnup for Core I

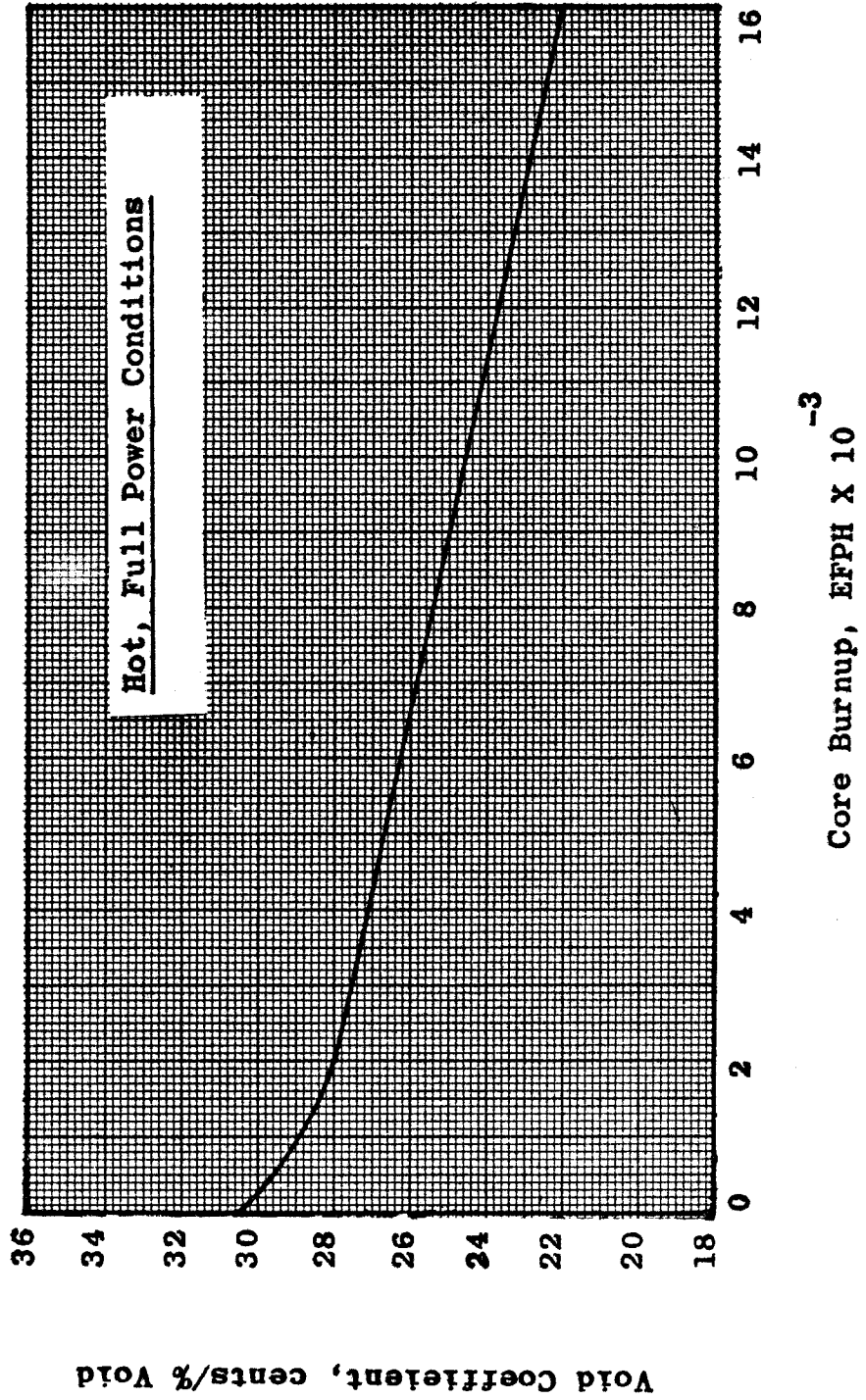


Figure 6-10. Operating Coefficient Variation with Burnup for Core I

